Supplement of Hydrol. Earth Syst. Sci., 21, 1593–1609, 2017
http://www.hydrol-earth-syst-sci.net/21/1593/2017/
doi:10.5194/hess-21-1593-2017-supplement

Hydrology and Earth System Sciences
Open Access
EGU

Supplement of

Can integrative catchment management mitigate future water quality issues caused by climate change and socio-economic development?

Mark Honti et al.

Correspondence to: Mark Honti (mark.honti@gmail.com)

Contents

S1 Detailed comparison of catchment and specialised models **S1**

S2 Model description **S3**
S2.1 Hydrology . . . S3
S2.2 Stream temperature . . . S3
S2.2.1 Shading . . . S4
S2.3 Pollutant hydrology . . . S4
S2.3.1 Urban Subsystem . . . S5
S2.3.2 Rural Subsystem . . . S7
S2.4 Transport of Particulate Matter . . . S7
S2.5 Traditional Pollutants . . . S7
S2.6 Dissolved Oxygen . . . S8
S2.7 pH . . . S8
S2.8 Biocides . . . S9
S2.9 Pesticides . . . S9

S3 Calibration results for PPPs **S10**

S4 Translation of management alternatives into boundary conditions or parameters **S11**
S4.1 BanBioc: Banning application of biocides on façades . . . S11
S4.2 StoreVol: Increasing storage volumes in urban drainage systems . . . S11
S4.3 PermPave: Increasing proportion of permeable pavements . . . S12
S4.4 RetRain: Retention of rainwater from roofs . . . S14
S4.5 WWTP: Enhancing WWTP treatment efficiency . . . S15
S4.5.1 Traditional pollutants . . . S15
S4.5.2 Organic micropollutants . . . S16
S4.6 OrgFarm: Exclusively organic farming . . . S17
S4.7 BufZone: Reconstruction of riparian buffer zones . . . S17
S4.7.1 Shading . . . S17
S4.7.2 Transport of pollutants . . . S17
S4.8 NatPark: Nature Park . . . S18
S4.9 Pollutant sources . . . S19
S4.10 Impact matrix of management alternatives . . . S19

S5 Predicted relative changes in pollutant quantiles **S21**

List of Figures

S1 Schema of flow-routing S5
S2 Calibration performance for PPPs not shown in Fig. 2 . . . . . S10
S3 Distribution of artificial landcover surfaces in the Mönchaltorfer Aa catchment S12
S4 Pavements of type B. S13
S5 Pavements of type C. S13
S6 Pavement type D S13
S7 Predicted relative changes in pollutant quantiles: climate S21
S8 Predicted relative changes in pollutant quantiles: socioeconomic scenarios S22
S9 Predicted relative changes in pollutant quantiles: management alternatives (I) S23
S10 Predicted relative changes in pollutant quantiles: management alternatives (II) S24
S11 Predicted relative changes in pollutant quantiles: management alternatives (III) S25

S1 Detailed comparison of catchment and specialised models

Features of selected existing catchment and small-scale models. iWaQa is the model developed in this study.

	AnnAGNPS	ANSWERS	CREAMS	GWLF	HSPF
Rural procedures					
Rural hydrology	Y	Y	Y	Y	Y
Erosion	Y	Y	Y	Y	Y
Nutrient loads	Y	Y	Y	Y	Y
Pesticide loads	Y	N	Y	N	Y
In-stream quality	N	N	N	N	Y
Urban procedures					
Urban hydrology	N	N	N	N	Y
CSO events	N	N	N	N	N
WWTP treatment	N	N	N	N	Y
Calculation					
Parameterization	Distributed	Distributed	Lumped	Lumped	Lumped
Time resolution	Dynamic	Dynamic	Dynamic	Dynamic	Dynamic
Spatial scale	Catchment	Catchment	Field?	Catchment	Catchment?
Resource requirement	High?	High?		Low	High?

	PhosFate	PRZM	SWAT	SWMM	iWaQa
Rural procedures					
Rural hydrology	Y	Y	Y	N	Y
Erosion	Y	Y	Y	N	Y
Nutrient loads	Y	N	Y	N	Y
Pesticide loads	N	Y	Y	N	Y
In-stream quality	N	N	Y	N	Partial
Urban procedures					
Urban hydrology	Y	N	Runoff	Y	Y
CSO events	N	N	N	Y	Y
WWTP treatment	N	N	N	Y	Y
Calculation					
Parameterization	Distributed	1D	Lumped	Structural	Lumped
Time resolution	Static	Dynamic	Dynamic	Dynamic	Dynamic
Spatial scale	Catchment	Field	Catchment	Catchment	Catchment
Resource requirement	Low	Low	High	High	Medium

References for models:

AnnAGNPS: Bingner, R. L., and F. D. Theurer. 2001. AnnAGNPS Technical Processes: Documentation Version 2.

ANSWERS original: Beasley, D. B., L. F. Huggins, and E. J. Monke. 1980. ANSWERS: A model for watershed planning. Trans. ASAE 23(4): 938-944.

ANSWERS dynamic: Bouraoui, F., I. Braud, and T. A. Dillaha. 2002. ANSWERS: A nonpoint-source pollution model for water, sediment, and nutrient losses. In: V. P. Singh and D. K. Frevert (eds.) Mathematical Models of Small Watershed Hydrology and Applications, 833-882. Highlands Ranch, Colorado: Water Resources Publications.

CREAMS: Knisel, W. G., ed. 1980. CREAMS: A field-scale model for chemicals, runoff, and erosion from agricultural management system. Conservation Research Report No. 26. Washington,D.C.: USDA-SEA.

GWLF: Haith, D.A. and L.L. Shoemaker, 1987. Generalized Watershed Loading Functions for Stream Flow Nutrients. Water Resources Bulletin, 23(3): 471-478.

HSPF: Donigian, A.S. Jr., B.R. Bicknell, and J.C. Imhoff. 1995. Hydrological simulation program - Fortran (HSPF). In: V. P. Singh (ed.) Computer Models of Watershed Hydrology, 395-442. Highlands Ranch, Colorado: Water Resources Publications.

PhosFate: Kovács Á, Honti M. and Clement A. (2008) Design of best management practice applications for diffuse phosphorus pollution using interactive GIS. Water Science and Technology 57: 1727-1733.

PRZM: Carsel R.F., L.A. Mulkey, M.N. Lorber, L.B. Baskin. 1985. The Pesticide Root Zone Model (PRZM): A procedure for evaluating pesticide leaching threats to groundwater, Ecological Modelling 30(1â2): 49-69. doi:10.1016/0304-3800(85)90036-5.

SWAT: Arnold, J. G., J. R. Williams, and D. R. Maidment. 1995. Continuous-time water and sediment-routing model for large basins. J. Hydraulic Eng. 121(2): 171-183.

SWMM: Metcalf and Eddy Inc., University of Florida, and Water Resources Engineers Inc., 1971, Storm Water Management Model, Vol. I. Final Report, 11024DOC07/71 (NTIS PB-203289), U.S. EPA, Washington, DC, 20460.

S2 Model description

S2.1 Hydrology

The modified LogSPM conceptual model (original model: Kuczera et al. (2006), modified version: Honti et al. (2014)) was used to simulate stream discharge. This conceptual model belongs to the family of saturation path models (hence the SPM abbreviation) that describe runoff formation by assuming a function that unambiguously maps between average soil moisture and saturated fraction of catchment surface. The model produces both total streamflow and individual flow components, namely baseflow, subsurface flow and runoff. A detailed description of the model and calibration procedure can be found in Honti et al. (2014).

References to section S2.1:

Honti M, Scheidegger A, Stamm C. (2014) Importance of hydrological uncertainty assessment methods in climate change impact studies. Hydrol. Earth Syst. Sci., 18, 3301–3317. doi:10.5194/hess-18-3301-2014

Kuczera G, Kavetski D, Franks S, Thyer M. (2006) Towards a Bayesian total error analysis of conceptual rainfall-runoff models: Characterising model error using storm-dependent parameters, Journal of Hydrology, 331, 161–177.

S2.2 Stream temperature

For modeling of stream temperature we used a simple first-order convergence model to the daily equilibrium temperatures following the concept of Edinger et al. (1968). The equilibrium temperature (T_{eq}) is the water temperature, at which the net heat flux between air and water is 0. This depends on the current meteorological conditions, so T_{eq} had to be calculated for each calculation unit, i.e. daily. The steady-state solution of the dynamic, process-based stream temperature model of Meier et al. (2003) was used to calculate T_{eq}. Following Mohseni & Stefan (1999) the net heat exchange through the air-water interface was assumed to be proportional to the difference between the actual water temperature (T) and T_{eq}. The proportionality constant k_T [MJ d^{-1} m^{-2} K^{-1}] accounts for all heat exchange processes in a lumped manner. The value of k_T varies with the meteorological conditions. It was estimated from the model of Meier et al. (2003) by establishing a multivariate linear regression between the actual heat exchange rates calculated by the dynamic model for a shallow water body, and meteorological variables influencing main heat exchange processes (shortwave radiation, air temperature, wind speed, relative humidity). The estimation of T_{eq} and k_T from a separate dynamic model would have allowed us to carry out heat exchange calculations for a stagnant water body in a very simple manner without compromising precision.

Since streams are not stagnant and they are organised in tree-like networks, heat transport exerts a huge influence on actual water temperatures at a specific monitoring site. Water parcels passing through a cross-section originate from different parts of the upstream catchment and thus have been exposed to heat exchange for different periods. To describe the complicated heat transport in a stream network in a tractable manner, we adopted the semi-Lagrangian approach of Yearsley (2009). This assumes plug flow (advection without longitudinal dispersion) in channels. The coupling of the simple first-order description of heat exchange with the plug flow assumption leads to the following stream temperature equation for a single water parcel:

$$T_{w,parcel}(\tau) = T_{eq} + \left(T_{source} - T_{eq}\right)\exp\left(-k_T \frac{\tau}{z}\right) \quad (1)$$

where τ is the travel time of the water parcel to the monitoring site, T_{source} is the initial water temperature at the beginning of travel in the stream network, and z is the water depth. T_{source} was estimated with the simple soil temperature model of Zheng et al. (1993). Equation (1) would only apply to cases with constant z. For a variable water depth the derivative of eq. (1) would have to be integrated along the water parcel's travel path with the actual location-dependent z. However, in small catchments of shallow streams the typical values of $k\tau/z$ are usually around or below 0.25. This allows for a reasonably precise estimation of the exponential part with a linear function of τ/z:

$$T_{\mathrm{w,parcel}}(\tau) \approx T_{\mathrm{eq}} + \left(T_{\mathrm{source}} - T_{\mathrm{eq}}\right)\left(1 - k_{\mathrm{T}}\frac{\tau}{z}\right) \tag{2}$$

The relative error of this approximation is below 2.5% if the exponent is not larger than 0.25. The linearity of eq. (2) with regard to τ/z allows the aggregation of the exposure coefficients of all water parcels coming from the upstream catchment into a discharge-weighted mean exposure value (X_{site}) for a specific monitoring point:

$$X_{\mathrm{site}} = \frac{\sum_i \left(q_i \sum_j \frac{\tau_{i,j}}{z_{i,j}}\right)}{\sum_i q_i} \tag{3}$$

where q_i is the flow per unit width of stream for each map cell i, whereas j refers to the spatial steps of the i^{th} water parcel from its source to the observation point. The discharge-weighted mean exposure coefficient represents the entire upstream network above an observation site and thus makes lumped calculation possible based on spatial aggregation of distributed data. T_{w} at the observation site can be calculated with a modified version of the water-parcel equation (1):

$$T_{\mathrm{w,site}}(t) = T_{\mathrm{eq}}(t) + \left(T_{\mathrm{source}}(t) - T_{\mathrm{eq}}(t)\right)\exp(-k_{\mathrm{T}}(t)X_{\mathrm{site}}) \tag{4}$$

The lack of time-dependence for X_{site} in eq. (4) assumes that discharge does not influence travel times and stage enough to change the exposure significantly.

S2.2.1 Shading

Shading influences the heat budget of water bodies most significantly by reducing incoming short-wave radiation. The estimation of the exact impact of shading in stream networks is complicated due to the involvement of travel time in heat transport. To remain simple, we used an 'effective shading ratio' k_{shade}. T_{eq} was calculated for the shaded case as well, with assuming a 90% reduction in incoming short-wave radiation. Then the applied equilibrium temperature was calculated by interpolating between the two equilibrium temperatures according to k_{shade}:

$$T_{\mathrm{eq,actual}} = k_{\mathrm{shade}}\, T_{\mathrm{eq,shade}} + (1 - k_{\mathrm{shade}})\, T_{\mathrm{eq}} \tag{5}$$

References to section S2.2:

Edinger JE, Duttweiler DW, Geyer JC (1968) The response of water temperatures to meteorological conditions. Water Resources Research 4: 1137-1143.

Meier W, Bonjour C, Wuest A, Reichert P (2003) Modeling the effect of water diversion on the temperature of mountain streams. Journal of Environmental Engineering: 755-764.

Mohseni O, Stefan HG (1999) Stream temperature/air temperature relationship: a physical interpretation. Journal of Hydrology 218: 128-141.

Yearsley JR (2009) A semi-lagrangian water temperature model for advection-dominated river systems. Water Resources Research 45: W12405.

Zheng D, Hunt RJ, Running SW (1993) A daily soil temperature model based on air temperature and precipitation for continental applications. Climate Research 2: 183-191.

S2.3 Pollutant hydrology

The needs of a model aiming to simulate water quality are usually different from the needs of a purely hydrological model. Due to the specific transport pathways of pollutants one needs to consider water fluxes that

are extremely important for the propagation of a given pollutant family but do not significantly contribute to streamflow. This means that – building on the modelled flow components – we have to use a more elaborate flow routing scheme that includes all important pollutant transport pathway but remains easily derivable from the catchment-scale flow components (baseflow, subsurface flow, runoff).

Since the majority of pollutants originate from the settlements and the agricultural areas, these subsystems deserve a more detailed hydrological description. From a hydrological perspective a general rural catchment's behaviour is dominated by the topsoils and the groundwater storage. Urban areas need to be relatively large to exert a detectable effect on the flow regime on the daily scale. Consequently, conceptual rainfall-runoff models typically lack a detailed urban hydrology module that would represent the different building blocks of the urban water infrastructure, as they would be anyway unidentifiable in the output. In the following sections we outline a complementary conceptual model framework that extends a general hydrological model with the necessary components for simulating contaminant transport.

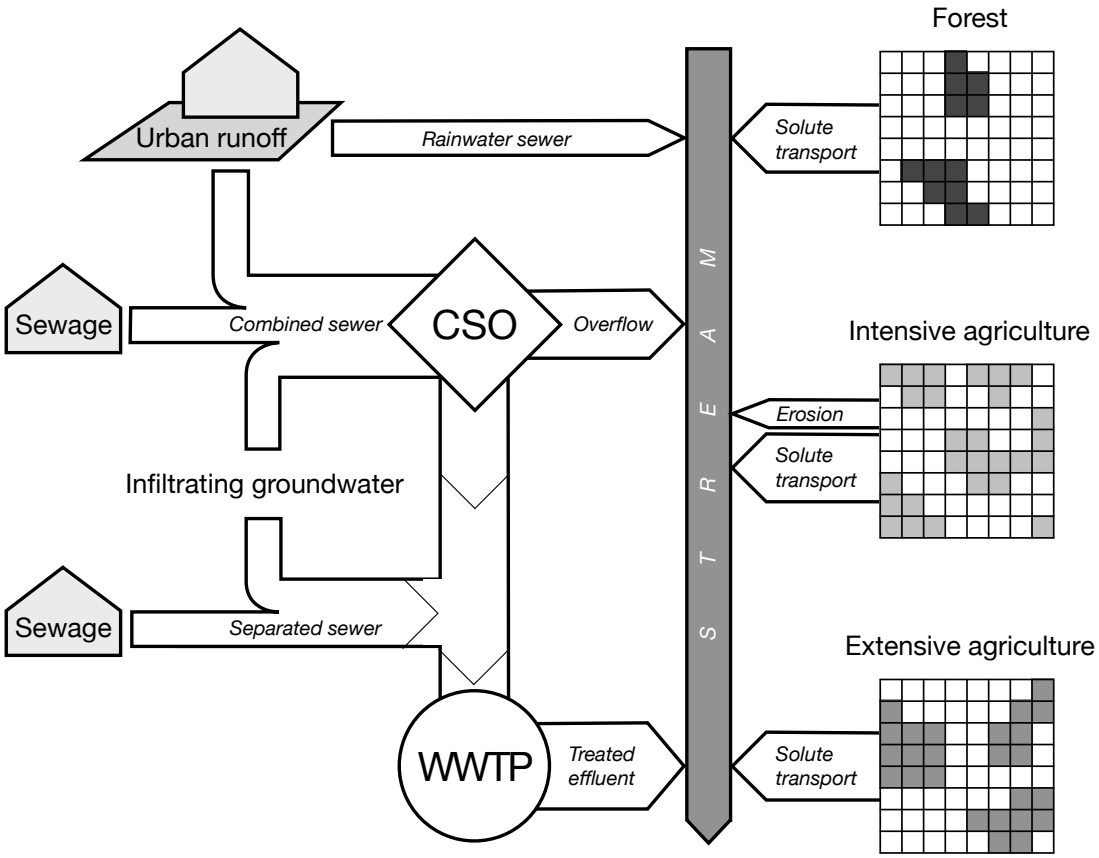

Figure S1: Schema of flow-routing

S2.3.1 Urban Subsystem

The total sewage production (Q_{sewage} [m^3 d^{-1}]) is considered to be steady and directly proportional to the number of people-equivalents (n_{PE}) connected to the sewer network:

$$Q_{\text{sewage}} = n_{\text{PE}} \cdot q_{\text{sewage}} \tag{6}$$

where q_{sewage} is the daily volume of sewage per PE [m^3 d^{-1}].

We assume that the amount of groundwater intrusion into the combined or purely wastewater sewers ($Q_{\text{parasitic}}$ [m^3 d^{-1}]) is proportional to the groundwater potential and thus indirectly to the amount of fast subsurface flow (Q_{ssf} [m^3 d^{-1}]):

$$Q_{\text{parasitic}} = k_{\text{ssf}} \cdot Q_{\text{ssf}} \tag{7}$$

where k_{ssf} is a simple proportionality factor [–].

In the same way, the storm-water input into combined sewers ($Q_{storm,comb}$) is a fixed proportion of the total runoff flux (Q_{runoff} [m^3 d^{-1}]):

$$Q_{storm,comb} = k_{runoff,comb} \cdot Q_{runoff} \tag{8}$$

while for the exclusively stormwater sewers:

$$Q_{storm,sep} = k_{runoff,sep} \cdot Q_{runoff} \tag{9}$$

The total hydraulic load of the combined sewer system is the amount of the sewage load connected to those sewers plus the storm-water input:

$$Q_{combined} = k_{comb} \cdot \left(Q_{sewage} + Q_{parasitic}\right) + Q_{storm,comb} \tag{10}$$

where k_{comb} [–] is the flow-proportional share of combined sewers.

Combined sewer overflows (CSO) occur when the hydraulic load of the combined sewer system exceeds the downstream transfer capacity for such a long period that the stormwater buffer tanks cannot retain the surplus for later withdrawal. Since the exact onset of CSO events depends on the actual dynamics of short-term rainfall and the hydraulics within the subcatchment and the sewer network, it is almost impossible to simulate these events with a model running on a coarse time-step. To overcome this obstacle we apply a "soft" approach on this naturally threshold-type problem. We assume that the probability of an overflow as the function of the hydraulic load is given by a smooth monotonic curve. The actual load forwarded towards the WWTP is:

$$Q_{intake} = \mathrm{SoftMin}(Q_{combined}, Q_{threshold}, k_{CSO}) \tag{11}$$

where $Q_{threshold}$ [m^3 d^{-1}] is the nominal forwarding capacity towards the WWTP and SoftMin is the soft minimum function (Cook 2011):

$$\mathrm{SoftMin}(Q_1, Q_2, k) = -\frac{\log(\exp(-kQ_1) + \exp(-kQ_2))}{k} \tag{12}$$

where the parameter k [–] determines the curvature of the function around the threshold.

Given the discharge forwarded to the WWTP, the discharge exiting as CSO (Q_{CSO} [m^3 d^{-1}]) is simply:

$$Q_{CSO} = Q_{combined} - Q_{intake}. \tag{13}$$

The total hydraulic load of the WWTP is the sum of the combined and separated input:

$$Q_{wwtp} = Q_{intake} + (1 - k_{comb})\left(Q_{sewage} + Q_{parasitic}\right) \tag{14}$$

The relative water residence time inside the WWTP (τ_{rel} [–]) is considered to be inversely proportional to the incoming flow:

$$\tau_{rel} = \frac{Q_{nominal}}{Q_{wwtp}} \tag{15}$$

where $Q_{nominal}$ [m^3 d^{-1}] is the nominal hydraulic load of the WWTP.

Rainwater sewers collect a specific proportion of total runoff and they emit to the streams directly:

$$Q_{storm,direct} = k_{runoff,direct} \cdot Q_{runoff} \tag{16}$$

References for section S2.3.1:

Cook J.D. (2011) Basic properties of the soft maximum. www.johndcook.com/soft_maximum.pdf. Accessed at 28/09/2015.

S2.3.2 Rural Subsystem

We assume that all discharge which doesn't come from the urban subsystem is originating from the rural parts of the catchment. The area-specific flow is then:

$$q_{\text{rural}} = \frac{Q_{\text{total}} - Q_{\text{wwtp}} - Q_{\text{cso}}}{A_{\text{rural}}} \tag{17}$$

The flow coming from a certain type of landuse (forest, intensive and extensive agriculture) is simply upscaled from the average flow by area:

$$Q_{\text{forest}} = q_{\text{rural}} \cdot A_{\text{forest}} \tag{18}$$

S2.4 Transport of Particulate Matter

Most of the erosion flux is caused by intensive precipitation, which is poorly known. So just like CSO events, daily erosion is difficult to model. Consequently, we try a simple empirical approach that follows the general dynamics but does not have many parameters that are difficult to identify. If we merge all the location-dependent factors, the revised USLE equation (USDA-ARS, 1992) can be replaced by a simple power function of the precipitation intensity:

$$f_{\text{erosion}}(t) = a_{\text{erosion}} \cdot P(t)^{b_{\text{erosion}}} \tag{19}$$

where $f_{\text{erosion}}(t)$ [kg SS km^{-2} d^{-1}] is the area-specific effective soil input to the stream network, $P(t)$ is the precipitation intensity [mm d^{-1}] and a_{erosion} and b_{erosion} are empirical parameters.

Based on the general vulnerability of different landuse categories to soil loss, we neglect erosion from forests and extensive agriculture and thus concentrate only on areas with intensive agriculture (arable land).

References for section S2.4:

USDA-ARS (1992) Revised Universal Soil Loss Equation 1.06 - Current Version. URL: http://www.ars.usda.gov/Research/d

S2.5 Traditional Pollutants

Traditional pollutants are present in most flow components of the model system. Therefore we can assign typical concentrations to these flow components and then calculate the corresponding inputs to the streams.

The effective treatment efficiency (K_{elim} [–]) in the WWTP depends on the relative residence time and air temperature (T_{air} [°C]):

$$K_{\text{elim}} = 1 - \exp\left(-\beta_{\text{elim}}\, \tau_{\text{rel}}\, \theta_{\text{elim}}^{T_{\text{air}}-20}\right) \tag{20}$$

where β_{elim} [–] is a logarithmic parameter determining the treatment efficiency of the WWTP at nominal hydraulic load and $T_{\text{air}} = 20\,°\text{C}$ and θ_{elim} [–] describes the temperature-dependence of the treatment process ($\theta_{\text{elim}} = 1$ means no temperature dependence).

The concentration of pollutant in the raw sewage is the product of the per capita daily emission (f_{person} [g d^{-1}]) and the daily sewage production (q_{sewage} [m^3 d^{-1}]):

$$C_{\text{sewage}} = \frac{f_{\text{person}}}{q_{\text{sewage}}} \tag{21}$$

The total flux leaving the WWTP (F_{wwtp} [g d^{-1}]) is then:

$$F_{\text{wwtp}} = (1 - K_{\text{elim}})\left(Q_{\text{tr,sewage}}\, C_{\text{sewage}} + Q_{\text{tr,storm}}\, C_{\text{storm}} + Q_{\text{tr,parasitic}}\, C_{\text{parasitic}}\right) \tag{22}$$

where the Q_{tr} terms correspond to the proportions of each flow component passing through the WWTP (assuming instant mixing in the sewer system).

The total untreated urban load (F_{untr} [g d^{-1}]) is the sum of the CSO output and the direct stormwater flux :

$$F_{\text{untr}} = Q_{\text{cso,sewage}} C_{\text{sewage}} + \left(Q_{\text{cso,storm}} + Q_{\text{direct,storm}}\right) C_{\text{storm}} + Q_{\text{cso,parasitic}} C_{\text{parasitic}} \tag{23}$$

The rural diffuse input (F_{diffuse} [g d^{-1}]) is the sum of the erosive and solute transports:

$$F_{\text{diffuse}} = A_{\text{agro,int}} m_{\text{erosion}} f_{\text{erosion}} + Q_{\text{agro,int}} C_{\text{agro,int}} + Q_{\text{agro,ext}} C_{\text{agro,ext}} + Q_{\text{forest}} C_{\text{forest}} \tag{24}$$

where m_{erosion} [g (g SS)$^{-1}$] is the mass of pollutant per unit soil dry weight.

Finally the total stream load (F_{stream} [g d^{-1}]) is the sum of all fluxes:

$$F_{\text{stream}} = F_{\text{wwtp}} + F_{\text{untr}} + F_{\text{diffuse}} \tag{25}$$

and then the in-stream concentration is:

$$C_{\text{stream}} = \frac{F_{\text{stream}}}{Q_{\text{total}}} \tag{26}$$

S2.6 Dissolved Oxygen

Analogously to the seasonally persistent pollutants, dissolved oxygen (DO) also has characteristic concentrations in different flow components, but mostly relative to the actual saturation level. We assume fixed concentrations for raw sewage, the WWTP effluent and infiltrating groundwater. We take fully saturated concentrations for all other flow components. The in-stream mechanisms are neglected due to the limited residence time.

S2.7 pH

Just like for DO, we assume characteristic pH and alkalinity (C_{alk}, [mg $CaCO_3$ l^{-1}]) in each flow component. Stream pH can be calculated by mixing all flow components. We follow the simplified procedure outlined in EPA's DESCON program (EPA 1988).

The logarithmic acid dissociation constant *pKa* is estimated from water temperature [°C] by empirical regression:

$$pKa = 6.57 - 0.0118\,T_{\text{w}} + 0.00012\,T_{\text{w}}^2 \tag{27}$$

The ionization fraction in each flow component depends on *pKa* and pH:

$$X_{\text{i}} = \frac{1}{(1 + 10^{pKa - pH})} \tag{28}$$

Total inorganic carbon of each flow component (C_{TIC}, [mg $CaCO_3$ l^{-1}]) comes then from alkalinity:

$$C_{\text{TIC,i}} = \frac{C_{\text{alk,i}}}{X_{\text{i}}} \tag{29}$$

The mixing of alkalinity and total inorganic carbon are calculated as for any other pollutant. The pH of the mixed flow becomes:

$$pH_{\text{mix}} = pKa - \log_{10}\left(\frac{C_{\text{TIC,mix}}}{C_{\text{alk,mix}}} - 1\right) \tag{30}$$

References for section S2.7:

EPA (1988) Technical guidance on supplementary stream design conditions for steady state modeling. US EPA Office of Water, Washington DC, USA.

S2.8 Biocides

Biocides need to possess a relatively large source stock so that they could exert a prolonged protective effect on building surfaces. This stock is continuously consumed by washout, transformations and ageing but in the same time it is also renewed by new constructions, and renovations. Although the mechanisms affecting biocide pollution could be described with the persistent source equations, we know relatively little about the available stock and its renewal rate. To avoid using too many poorly defined parameters we use a simplified version that relies on a unit stock per facade area. The total flux from the buildings ($F_{\text{buildings}}$ [g d^{-1}]) is the product of the biocide-treated area (A_{bioc} [km^2]), precipitation (P [mm d^{-1}]), a washout rate (β [mm^{-1}]) and the available stock itself (M_{stock} [g km^{-2}], at present = 1):

$$F_{\text{buildings}} = \beta \cdot A_{\text{bioc}} \cdot P \cdot M_{\text{stock}} \tag{31}$$

This flux goes into two directions: a certain part is emitted directly into the streams via rainwater sewers and via CSO overflows. For the part passing through a WWTP a constant removal efficiency was assumed, as neither ozonation nor PAC addition depend on the residence time within the WWTP.

S2.9 Pesticides

Agricultural pesticides are less persistent in the environment than biocides and they are usually applied in well-defined stages of crop development. These properties commonly result in seasonally variable environmental availability and concentrations. Timing is crucial, time differences between the application period and the next few storm events determine the magnitude of concentration peaks. To predict pesticide pollution in the future climate we need to parameterize the application algorithm instead of using fixed application dates.

A certain amount of pesticide (m_{applic} [g km^{-2}]) is allocated for the relevant crop for each year. We calculate a heat sum (T_{sum} [°C d]) from the beginning of the year. Once the target heat sum (T_{target} [°C d]) is reached, application (f_{applic} [g d^{-1} km^{-2}]) is carried out on each dry day (with $P < P_{\text{threshold}}$) with a certain daily allowance (f_{daily} [g d^{-1} km^{-2}]) until the allocated stock is completely used up.

The available field stock (M [g]) of the pollutant is calculated with a dynamic mass balance:

$$\frac{\mathrm{d}M}{\mathrm{d}t} = f_{\text{applic}} \cdot A_{\text{crop}} - k_{\text{transform}} \cdot M \cdot \theta_{\text{transform}}^{T_{\text{air}}-20} - F_{\text{transport}} \tag{32}$$

where A_{crop} [km^2] is the cultivation area of the relevant crop, $k_{\text{transform}}$ [d^{-1}] is the rate of transformation at 20 °C, $\theta_{\text{transform}}$ [–] describes the temperature dependence of transformation and $F_{\text{transport}}$ [g d^{-1}] is the transported flux:

$$F_{\text{transport}} = \beta_{\text{transport}} \cdot Q_{\text{fast}} \cdot M \tag{33}$$

where $\beta_{\text{transport}}$ [m^{-3}] is the driver-specific loss rate to the streams and Q_{fast} [m^{-3} d^{-1}] is the sum of runoff and subsurface flow from the application area.

The final stream concentration is the total transported flux divided by discharge:

$$C_{\text{stream}} = \frac{\sum_i F_{\text{transport},i}}{Q_{\text{total}}} \tag{34}$$

S3 Calibration results for PPPs

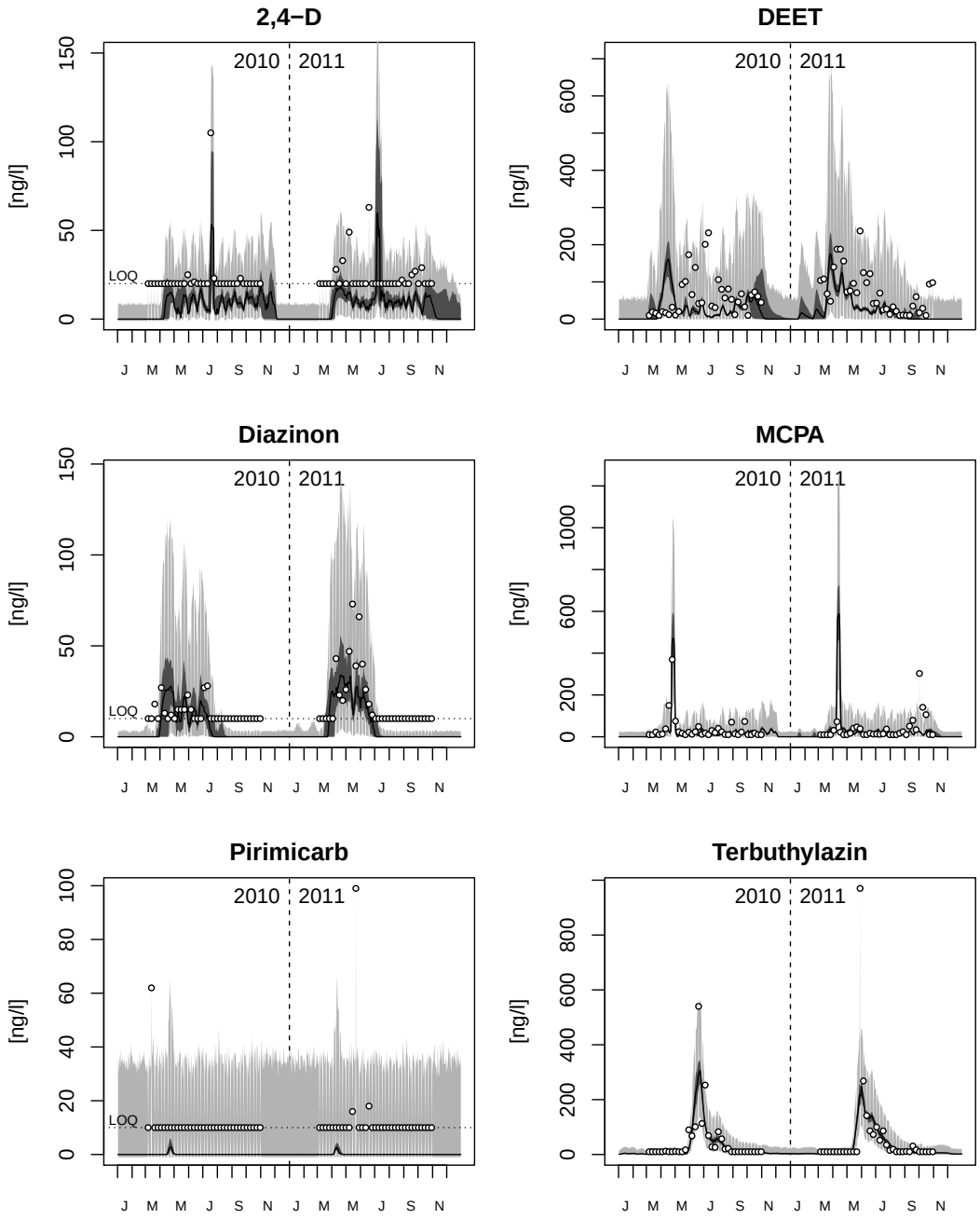

Figure S2: Calibration performance for PPPs not shown in Fig. 2. Dots are observations, black line is the model simulation with maximum posterior probability parameters, the dark and light grey regions are the 95% parametric and total uncertainty intervals, respectively. All values are weekly mean concentrations; detection limits were 10 ng L^{-1} for all compounds, except 2,4-D (20 ng L^{-1}).

S4 Translation of management alternatives into boundary conditions or parameters

The following management alternatives were considered in our study:

- Urban measures

  BanBioc Banning application of biocides on façades.

  StoreVol Increasing storage volumes in urban drainage systems.

  PermPave Increasing proportion of permeable pavements.

  RetRain Retention of rainwater from roofs.

  WWTP Enhancing WWTP treatment efficiency

- Agricultural measures

  OrgFarm Exclusively organic farming.

  BufZone Reconstruction of riparian buffer zones.

  NatPark Nature Park.

These measured were formulated on different levels between precise technical specifications and purely administrative directives, so they could not be directly used as modified boundary conditions for our model. Therefore, management alternatives had to be translated into exact technical terms prior to modeling their impacts.

S4.1 BanBioc: Banning application of biocides on façades

Specification: Currently biocides are used in façade paints to prevent the growth of biofilms that would impair the appearance of façades. This alternative assumes a complete ban of biocides (diuron and terbutryn from our compound list) in façade paints.

Translation: We assume that the banned biocides are not applied anymore in façade paints and that the presently existing stocks are depleted before the future prediction period (2036-2064). So these biocides will not be present in the (model) environment at all.

S4.2 StoreVol: Increasing storage volumes in urban drainage systems

Specification: The measure aims at reducing the volume and frequency of untreated combined sewage loads into the streams.

Translation: Buffers are designed according to design guidelines, resulting in similar tank size per catchment area. Unfortunately, neither the actual buffer sizes nor the applied design guidelines were known by us. To overcome the lack of data, we estimated CSO operation from empirical data. There are characteristic numbers on typical operating frequencies and durations from Portmann (2011) for a location on the Swiss Plateau [table data from Weiss et al. (2006), gray shading shows statistics for the CSO Vogelberg]:

overflow frequency [events year^{-1}]		overflow duration [hours year^{-1}]	
0 – 15	very rare	0 – 20	very short
15 – 43	rare	20 – 163	short
43 – 88	average	163 – 308	average
88 – 159	frequent	308 – 644	long
> 159	very frequent	> 644	very long

Based on these data we assume that a standard CSO tank in the study area overflows about 40 times a year with about 300 hours of active time. In the management alternative we assume that buffers are enlarged to twice their original sizes. This should reduce overflow duration and frequency.

To estimate the effect of enlarged CSOs we calibrate a double-linear reservoir fed by 10-minute rainfall data from MeteoSchweiz location Zürich Fluntern to match the target overflow times and frequencies. The calculated annual overflow statistics with standard and double storage volumes are the following:

Size	Total overflow [mm year^{-1}]	Overflow proportion [–]	Event duration [hrs year^{-1}]	Event frequency [events year^{-1}]
Standard	236	21%	304	37
Double	145	13%	154	18

References to section S4.2:

Weiss G.,H. Brombach, Ch. Wöhrle (2006) Monitoring of Combined Sewer Overflow Tanks: Results of 500 Years of Measurement Records. Water Practice and Technology doi:10.2166/wpt.2006.011

S4.3 PermPave: Increasing proportion of permeable pavements

Specification: Paved areas increase urban runoff and therefore converting presently impermeable surface pavements with more permeable types helps to reduce flash floods, and wash-off of urban diffuse pollution.

Translation: Paved areas subject to light or moderate physical stress will be converted into permeable surfaces to increase infiltration and to decrease urban runoff. The distribution of paved surfaces (576 ha) in the Mönchaltorfer Aa catchment is shown on Fig. S3.

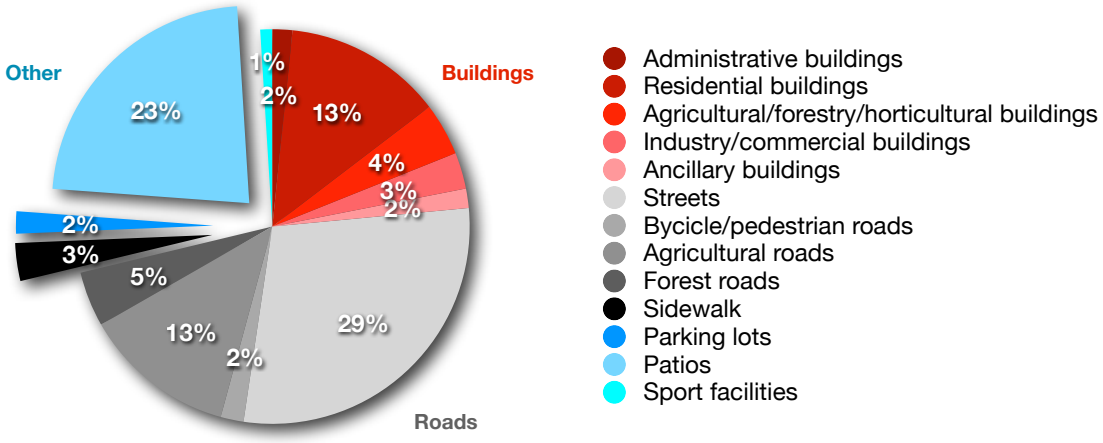

Figure S3: Distribution of artificial land cover types in the Mönchaltorfer Aa catchment.

There are 10.3 ha parking lots and 17.6 ha of sidewalks in the catchment communities (GIS data source: Kanton ZH). Besides the normal roads the 2nd biggest area are the patios – paved areas around buildings (*Hausumschwung*). This area justifies why it is reasonable to include this pavement category in the planned measures.

There are different kinds of pavements with regard to permeability. Those designed for more frequent traffic (like parking lots of shops, etc.) are more durable but in the same time less permeable to rainfall.

A: Standard impermeable pavement The maximal surface storage is about 1 – 1.5 mm of water, which means that rainfall events with smaller intensity would not cause any runoff. Since the pavement is impermeable, the surface storage is depleted by evaporation alone.

B: Concrete tiles with permeable grout (Fig. S4) The more granular surface and the small depressions above the grout increase the maximal surface storage to 2.5 mm. The grout is typically filled with sand, so it has a permeability of about 15 – 20 mm/h. As this surface is intended for lots with frequent traffic, the grout occupies a small fraction of the total area (about 5%).

C: Concrete grid blocks with grass (Fig. S5) This type is designed for permanent parking lots that have sparse traffic (few cars per day). The permeable material covers a significant portion of the total area (30 – 50%). The permeability is partially reduced compared to clean sand due to the finer-grained filling material that is required to maintain the plant coverage. The soil level in the holes is typically lower due to the compression effect from the tyres, so the maximal storage capacity increases to about 3 – 3.5 mm.

D: Plastic reinforcement grid for lawns (Fig. S6) Some lawn areas occasionally serve as parking lots or are exposed to car traffic in an other way. This plastic grid helps to distribute the pressure from the tyres over a larger area and resists the shear stress caused by accelerations, turns and braking. The overall permeability is similar to lawns because the plastic grid occupies only a small fraction of the area.

Figure S4: Pavements of type B.

Figure S5: Pavements of type C.

Figure S6: Pavement type D during installation (left) and inside the lawn (right).

Permeability coupled with the increased storage capacity means that these surface types produce less runoff compared to the impermeable pavement. However, this reduction appears mostly during precipitation events having a lower rainfall intensity. High-intensity rainfall quickly fills the available surface storage and produces runoff from most of the total rainfall. This means that although runoff is less frequent from these surfaces, the average intensity of runoff events is higher compared to impermeable pavements. This means that these surfaces are subject to pollutant deposition–flush cycles.

The annual mean runoff formation by pavement type (based on past SMA precipitation data, 1105 mm [MeteoSchweiz]) was the following:

Pavement type	Storage capacity [mm]	Infiltration capacity [mm h^{-1}]	Runoff [mm]	Runoff prop. [–]	Mean runoff intensity [mm h^{-1}]
A	1	0	843	76%	0.49
B	2	1	312	28%	0.82
C	3	7	35	3%	2.16

The applicability of pavement types depends on the magnitude of traffic stress, which in turn is related to population density. We draw the threshold at 6000 ind. km^{-2} for the application of pavement type C in parking lots and for type B in sidewalks and patios.

The proposed measures for increasing urban permeable surfaces are the following:

Scenario	Pop. density [ind km^{-2}]	Sidewalks	Parking lots	Patios
Present	4750	100% A (17.6 ha)	100% A (10.3 ha)	100% A (130 ha)
Status quo	4750	100% B (17.6 ha)	50% B (5.15 ha), 50% C (5.15 ha)	100% C (130 ha)
Moderate growth	5420	100% B (18.5 ha)	50% B (5.45 ha), 50% C (5.45 ha)	100% C (136 ha)
Exploding growth	9770	100% A (69 ha)	100% B (40.2 ha)	100% A (506 ha)
Decline	4750	100% B (17.6 ha)	50% B (5.15 ha), 50% C (5.15 ha)	100% C (130 ha)

As a preliminary estimation of the impact of this alternative we calculated the mean urban runoff from the entire catchment in the different socio-economic scenarios:

Scenario	Mean urban runoff with converting patios [L s^{-1}]	Mean urban runoff without converting patios [L s^{-1}]
Present	136	136
Status quo	98	131
Moderate growth	103	138
Exploding growth	525	525
Decline	98	131

S4.4 RetRain: Retention of rainwater from roofs

Specification: Rainwater should be collected from roofs and diverted from stormwater sewers to infiltration facilities to reduce urban runoff and increase groundwater recharge in urban areas.

Translation: Current Swiss law requires infiltration of rainwater, so the improvement of rainwater retention is not only a theoretical storyline for the future.

The case study area has limited infiltration capacity according to a report by Hunziker-BetaTech (2009). The main reasons are that most of the settlements are situated in places where the groundwater level is naturally high and that the soil hydraulic properties at the flat areas do not really favour infiltration.

The assumptions used to estimate the necessary green area for infiltration were the following:

Infiltration capacity:	1 L m^{-2} min^{-1}
Infiltration area/roof area:	1/20
Maximal retention depth:	0.6 m

This means that for a roof area of 200 m^2 there would be a 10 m^3 infiltration area with 6 m^3 retention volume. The area-specific infiltration capacity means that there is the theoretical possibility to infiltrate 72 mm of rainwater in a single day. On the other hand, the buffer can accommodate for 30 mm of rainfall (on the roof area) without any infiltration. The rainfall intensities with about 3 years of return period are around 18 and 20 mm for the 10-30 minutes duration domain.

These figures indicate that such an infiltration system can completely infiltrate the runoff from the roof. Overflow events will occur with very low probability (return period $\geq$ 3 years).

According to the estimates of Hunziker-BetaTech (2009), the current infiltration capacity is already utilised by approximately 5% of the present roof area, so extra technical efforts are needed to improve the situation.

Grades of infiltration in socio-economic scenarios:

Scenario	Roof area connected to infiltration	Infiltration area requirement (1/20 of roof area)
Present	5% (6.8 ha)	0.34 ha
Status quo	20% (27.2 ha)	1.36 ha
Moderate growth	20% (28.6 ha)	1.43 ha
Exploding growth	20% (106.0 ha)	5.30 ha
Decline	20% (27.2 ha)	1.36 ha

Due to the efficiency of the infiltration system the connected roof area specifies the relative amount of drained roof runoff:

Scenario	Roof area connected to sewers	Total drained roof runoff
Present	95% (129 ha)	45 l/s
Status quo	80% (109 ha)	38 l/s
Moderate growth	80% (114 ha)	40 l/s
Exploding growth	80% (424 ha)	148 l/s
Decline	80% (109 ha)	38 l/s

References for section S4.4:

Hunziker-BetaTech (2009) Assessment of the potential to infiltrate stormwater in the municipalities of Egg, Grüningen, Mönchaltorf and Gossau ZH for the NRP61 SWIP project (in German), Winterthur, Switzerland.

Portmann, A. (2011) Evaluation of the performance of combined sewer overflow tanks (in German). B.Sc. thesis, Department of Urban Water Management, IfU, ETH Zurich, Zurich, Switzerland.

S4.5 WWTP: Enhancing WWTP treatment efficiency

Specification: WWTPs should be upgraded by adapting enhanced treatment technologies to keep more pollutants away from streams.

Translation: The removal of traditional and micropollutants requires different technologies. These are explained in the following subsections.

S4.5.1 Traditional pollutants

Low-load activated sludge plant with separate reactor for denitrification and preliminary P precipitation (Somlyódy et al. 2002; Henze & Odegaard, 1994; Zessner et al. 1999):

Parameter	Nominal removal rate**	Typical concentrations
BOD	95%	$BOD_{in} \sim 250$ mg/l $BOD_{out} \sim 12$ mg/l
TN	85%	$TN_{in} \sim 48$ mg/l NH4-$N_{out} \sim 0$ mg/l, NO3-$N_{out} \sim 7$ mg/l
TP	95%	$TP_{in} \sim 12$ mg/l, $TP_{out} \sim 0.6$ mg/l

** at nominal hydraulic residence time

References to section S4.5.1:

Henze M., Odegaard H. (1994) An analysis of wastewater treatment strategies for Central and Eastern Europe. Water Science & Technology. 30(5).

Somlyódy L., Shanahan P. (1998) Municipal wastewater treatment in Central and Eastern Europe. Present situation and cost-effective development strategies. The World Bank, Washington DC.

Zessner M., Fenz R, Kroiss H. (1999) Waste water management in the Danube Basin. Water Science & Technology 38(11).

S4.5.2 Organic micropollutants

Removal efficiencies for micropollutrants with ozonation or PAC:

Substance	Biological treatment	+ nitrification	O_3	PAC	Proposed value
Atrazine	40%[1]	10%[1]	60%[2], 45%[8], >90%[11]		60%
Metolachlor			82%[8]		80%
Isoproturon	25%[1]	55%[1]	>99%[6,10]		99%
Diuron	0%[3]	60%[9]	74%[6]	80%[3], 90%[3]	80%
Mecoprop	20%[1]	15%[1]	85%[2], 79%[6]	65%[3]	80%
Terbutryn	35%[1]	50%[1]	>89%[6], >99%[7,10]	77%[3], 85%[3]	95%
2,4-D			>80%[7], >90%[11]		90%
DEET		70%[5]	80%[5], 62%[6], 78%[8]		80%
Diazinon			72%[6], >90%[7]		90%
MCPA	5%[4]		77%[4], 75%[6], >99%[7,11]		80%
Pirimicarb					80%
Terbuthylazin			52%[7]		50%

References for removal efficiencies in the above table:

1. Abbeglen C., Mikroverunreinigungen in Kläranlagen, gwa 7/2010, p. 587-594, 2010.
2. BAFU, Mikroverunreinigungen aus kommunalem Abwasser, Report Nr: UW-1214-D, Bundesamt für Umwelt BAFU, 2012ă
3. Boehler M., B. Zwickenpflug, J. Hollender, T. Ternes, A. Joss and H. Siegrist, Removal of micropollutants in municipal wastewater treatment plants by powder-activated carbon. 2012 Water Science & Technology 66.10, 2115-2121, doi: 10.2166/wst.2012.353
4. Reungoat J., M. Macova, B.I. Escher, S. Carswell, J.F. Mueller, J. Keller, Removal of micropollutants and reduction of biological activity in a full scale reclamation plant using ozonation and activated carbon filtration. Water Research, Volume 44, Issue 2, January 2010, Pages 625–637. http://dx.doi.org/10.1016/j.watres.2009.09.0 [Dose: 0.5ămg O_3 mg DOC^{-1}]
5. Sui Q., J. Huang, S. Deng, G. Yu, Q. Fan, Occurrence and removal of pharmaceuticals, caffeine and DEET in wastewater treatment plants of Beijing, China. Water Research, Volume 44, Issue 2, January 2010, Pages 417-426. http://dx.doi.org/10.1016/j.watres.2009.07.010 [ozone dosage: 5ămg L^{-1}, contact time: 15 min]
6. Hollender Juliane, Saskia G. Zimmermann, Stephan Koepke, Martin Krauss, Christa S. McArdell, Christoph Ort, Heinz Singer, Urs von Gunten and Hansruedi Siegrist. Elimination of Organic Micropollutants in a Municipal Wastewater Treatment Plant Upgraded with a Full-Scale Post-Ozonation Followed by Sand Filtration. Environ. Sci. Technol., 2009, 43 (20), pp 7862–7869 [ozone dosage: 0.6 mg O_3 / mg DOC]
7. Ikehata Keisuke & Mohamed Gamal El-Din, Aqueous Pesticide Degradation by Ozonation and Ozone-Based Advanced Oxidation Processes: A Review (Part I & II), Ozone: Science & Engineering: The Journal of the International Ozone Association Volume 27, Issues 2 & 3, pages 83-114 & 173-202, 2005, DOI:10.1080/019195105 & 10.1080/01919510590945732
8. Lei Hongxia, Shane A. Snyder, 3D QSPR models for the removal of trace organic contaminants by ozone and free chlorine, Water Research, Volume 41, Issue 18, October 2007, Pages 4051-4060, http://dx.doi.org/10.1016/j.watr

9. Rosal R., A. Rodríguez, J. A. Perdigón-Melón, A. Petre, E. García-Calvo, M. J. Gómez, A. Agüera, A. R. Fernández-Alba, Occurrence of emerging pollutants in urban wastewater and their removal through biological treatment followed by ozonation Water Research, Volume 44, Issue 2, January 2010, Pages 578-588 http://dx.doi.org/10.1
10. Roche, M. Prados, Removal Of Pesticides By Use Of Ozone Or Hydrogen Peroxide/Ozone, Ozone: Science & Engineering Vol. 17, Iss. 6, 1995 [ozone dosage: 1 mg/mg DOC]
11. Meijers T., E. Oderwald-Muller, P. A.N.M. Nuhn, J. C. Kruithof Degradation of Pesticides by Ozonation and Advanced Oxidation, Ozone: Science & Engineering Vol. 17, Iss. 6, 1995 [ozone dosage: 1.2-1.5 mg/mg DOC]

Based on the large variation in published removal efficiencies, we took a flat rate of 80% for all compounds and treatment technologies.

S4.6 OrgFarm: Exclusively organic farming

Specification: Agriculture will be converted to organic farming in the entire catchment.

Translation: The aim is to reduce the losses of organic synthetic pesticides from the fields. This means that the application of organic synthetic agricultural pesticides ceases in the entire catchment.

S4.7 BufZone: Reconstruction of riparian buffer zones

Specification: Riparian buffer zones will be reconstructed to retain diffuse pollution from streams and to increase shading.

Translation: The aim is to reduce summer water temperatures, reduce the transportation of particulate and dissolved pollutants from the fields and to restore ecological habitats along the streams. The details on shading and nutrient retention are discussed in the following subsections.

S4.7.1 Shading

Currently 28% of the stream network in the Western subcatchment is situated in forests. Forested proportions are 5.5 and 6.5% in the Central and Eastern subcatchments, respectively. So the current shading efficiency is quite low in the catchment. The restoration of tree-stocked buffer zones would increase shading and thus decrease summer water temperatures significantly.

The shading efficiency of trees varies by type, season, stream width and channel orientation. The maximum posterior likelihood value for the shading efficiency was 0.18 for Western subcatchment. This indicates that there is no 100% shading efficiency even with full forest coverage. We will use the ratio of effective shading and forest coverage (18% / 28% $\approx$ 65%) as the highest shading efficiency.

Thus, the reconstruction of riparian buffer zones would increase the shading efficiency to 65% in all non-urban stream sections (along 38.3 km from the 67.9 km total length).

S4.7.2 Transport of pollutants

The travel time of water and thus the transported particles through a buffer zone depends on the effective roughness of the surface. This is mainly shaped by vegetation. Dense natural grasslands and dense deciduous forests with a natural undergrowth typically have Manning's roughness coefficients of n = 0.20 and 0.60 (for sheet flow), respectively. In contrast, short grass has 0.15 and bare earth has 0.02.

The mean flow velocity is inversely proportional to n, so one can calculate the relative travel time increment achieved by the buffer zone.

Bank vegetation	Manning's n	Relative travel time
Short grass	0.15	1.00
Long grass with weeds	0.20	1.33
Trees with dense undergrowth	0.60	4.00

It is obvious from the above values that it is only the forested buffer zone that can achieve a significant increase in travel time. The exact retention depends on the width and slope of the buffer zone and the distribution of the pollutant between the dissolved and particulate-bound phases.

The retention of particles is usually modeled with first-order kinetics, so the retention depends exponentially on time. Considering a buffer width of 5 m with a slope of 1% and a hydraulic radius of 5 mm for sheet flow, and a particle retention coefficient of 0.001 [1/s] (typical value for Austrian catchments [Kovács et al. 2012]), the absolute travel times and retention efficiencies become the following:

Bank vegetation	Manning's n	Sheet flow velocity [cm s^{-1}]	Travel time [s]	Retention efficiency
Short grass	0.15	1.9	257	23%
Long grass with weeds	0.20	1.5	342	29%
Trees with dense undergrowth	0.60	0.5	1026	64%

This gain in retention can quickly diminish if the buffer zone is too narrow, too inclined or the vegetation is too sparse.

The available area for the buffer strips depends on the legally defined Gewässerraum. This is altogether 11 m for streams with less than 2 m natural channel bottom width (CBW) and [2.5 x CBW + 7] m for 2 m < CBW < 15 m. A low-order stream with about 1 m CBW would then possess 5 m wide buffer strip on each side. This means that the achievable retention is rather low for the most abundant stream types, which receive the majority of diffuse loads. A high-order stream with for example 5 m CBW would get 19.5 m Gewässerraum, but due to the space requirement of bank slopes (usually having 1:1.5 to 1:2 inclination, so a 2 m deep ditch requires 6 to 8 m for the bank slopes alone) the effective (moderately inclined) retention area is similar or even smaller compared to low-order streams.

The retention efficiency cannot be directly combined with the total (mobilized) load. Based on results from different catchments in the region (e.g. Frey et al. 2009), a substantial fraction of the catchment drains into internal sinks (50 - 80%). Hence, the buffer strips can retain only a fraction of the total load corresponding to an estimate of 20 - 50% of connected areas.

Retention will not significantly increase for dissolved pollutants, because the retention coefficients are much smaller. This means that retention is more like a linear function of travel time. Since the overall time spent in the buffer zone is relatively short to the total travel time from the field to the stream, no big improvement can be expected, unless there is a special mechanism that retains the pollutant much faster in the buffer zone (like nutrient uptake of plants).

References to section S4.7.2:

Frey, M., A. Dietzel, M. Schneider, P. Reichert, and C. Stamm. (2009) Predicting critical source areas for diffuse herbicide losses to surface waters: role of connectivity and boundary conditions. Journal of Hydrology 365:23-36.

Kovacs A., Honti M., Zessner M., Eder A., Clement A., Blöschl G. (2012) Identification of phosphorus emission hotspots in agricultural catchments. Sci. Tot. Env. 433:77-88.

S4.8 NatPark: Nature Park

Specification: The entire catchment would be converted into a nature park.

Translation: The application of agrochemicals ceases in the catchment. This means that exposure to all agrochemicals would decrease to natural background levels.

S4.9 Pollutant sources

Pollutants originate from different sources in the catchment. The source matrix for the CurrPrac management alternative is as follows:

	Urban area					Intensive agriculture						
	Inhabitants	Façades	Bitumen sheets	Gardens	Other/generic	Corn	Cereals	Sugarbeet/vegetables	Fruits	Other/generic	Extensive agriculture	Forest
NO_3	■				■					■	■	■
SO_4	■				■					■	■	■
Cl	■				■					■	■	■
PO_4	■				■					■	■	■
NH_4	■				■					■	■	■
atrazin						□						
isoproturon							□					
metolachlor						□		□				
2,4-D						□	□					
DEET										□		
diazinon									□		□	
MCPA							□				□	
pirimicarb									□			
terbuthylazin						□						
diuron		□										
mecoprop			■	■								
terbutryn		□										

Closed symbols (■) indicate sources that apply in all management alternatives, open symbols (□) stand for sources that differ by alternative (being active in CurrPrac). The BanBioc, OrgFarm, NatPark, and the All management alternatives change the source matrix by the complete elimination of diuron/terbutryn (in BanBioc and All) and the banning of all agrochemicals (in OrgFarm, NatPark, and All).

Socio-economic scenarios influence the sources via the area covered by specific landuse classes, the number inhabitants and total façade area in the catchment.

S4.10 Impact matrix of management alternatives

The theoretical impact matrix of management alternatives can be constructed based on the model structure. Closed symbols (■) indicate a direct mechanistic relationship between a management alternative and a corresponding water quality parameter. Open symbols (□) for the PermPave and RetRain alternatives indicate indirect impacts on pollutant concentrations via the reduction of urban runoff.

	BanBioc	StoreVol	PermPave	RetRain	WWTP	OrgFarm	BufZone	NatPark	All
discharge			■	■				■	■
T_w							■		■
NO_3		■	□	□	■			■	■
SO_4		■	□	□				■	■
Cl		■	□	□				■	■
PO_4		■	□	□	■			■	■
NH_4		■	□	□	■			■	■
atrazin						■	■	■	■
isoproturon						■	■	■	■
metolachlor						■	■	■	■
2,4-D						■	■	■	■
DEET						■	■	■	■
diazinon						■	■	■	■
MCPA						■	■	■	■
pirimicarb						■	■	■	■
terbuthylazin						■	■	■	■
diuron	■	■	□	□	■				■
mecoprop		■	□	□	■				■
terbutryn	■	■	□	□	■				■

S5 Predicted relative changes in pollutant quantiles

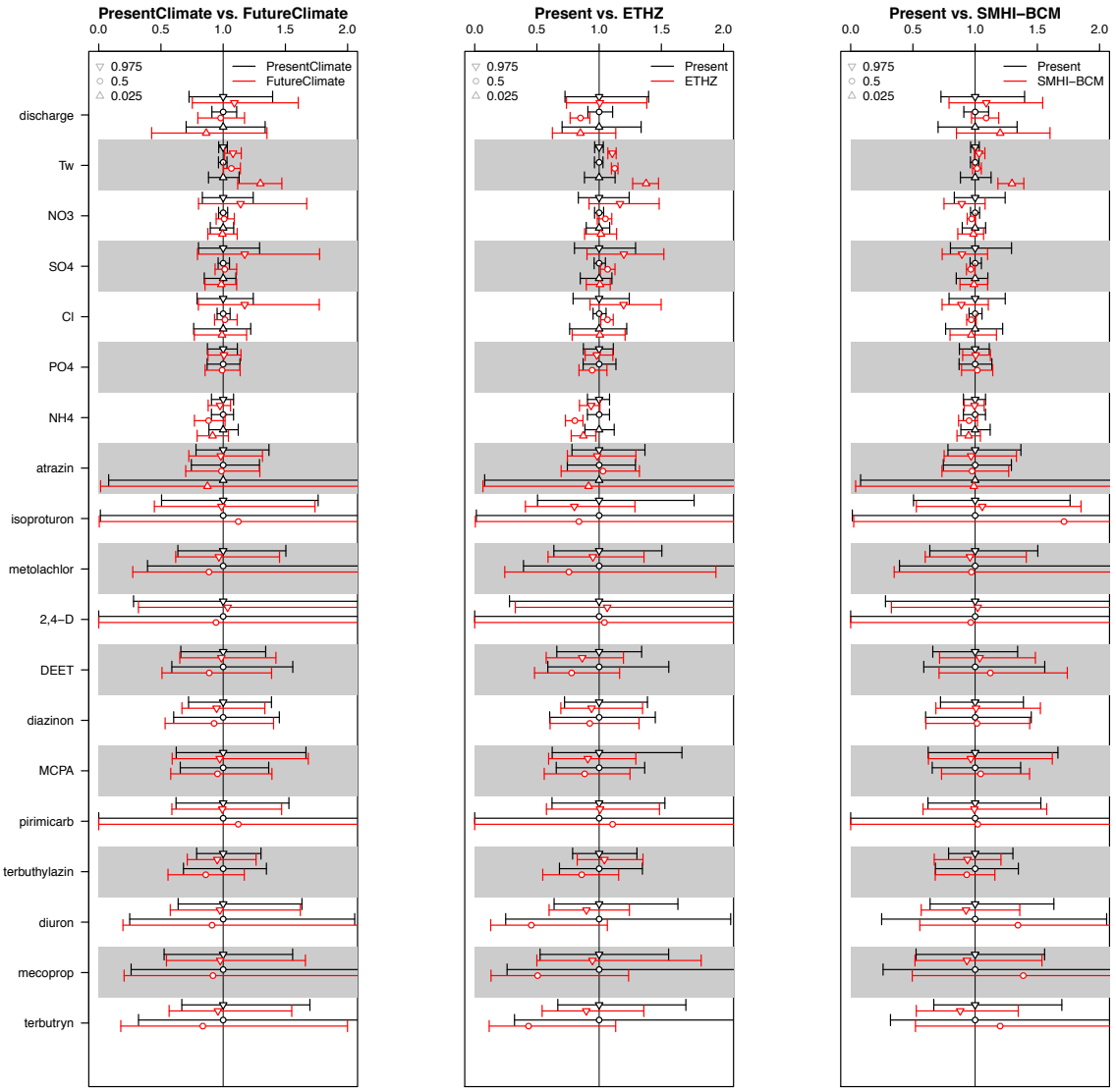

Figure S7: Relative change for high (Q97.5%), median (Q50%) and low (Q2.5%) quantiles of predicted model variables. FutureClimate is the uncertain future climate reflected by the ensemble of 10 GCM-RCM chain predictions. Unless otherwise stated, all simulations used present climate + StatusQuo + CurrPrac. Missing low quantiles correspond to cases where a present expected value of 0 for the low quantile prevented the meaningful normalisation of values.

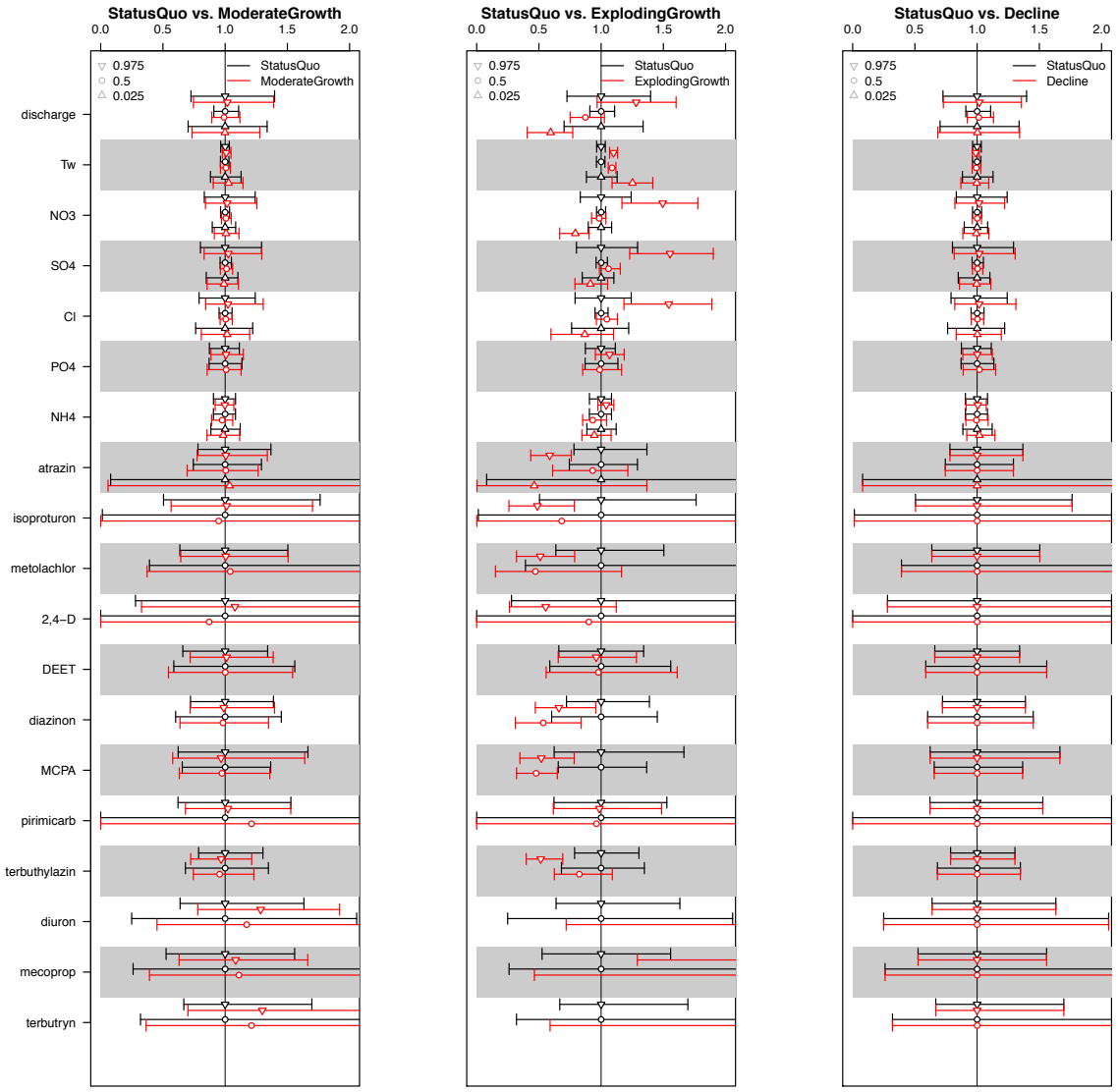

Figure S8: Relative change for high (Q97.5%), median (Q50%) and low (Q2.5%) quantiles of predicted model variables. Unless otherwise stated, all simulations used present climate + StatusQuo + CurrPrac. Missing low quantiles correspond to cases where a present expected value of 0 for the low quantile prevented the meaningful normalisation of values.

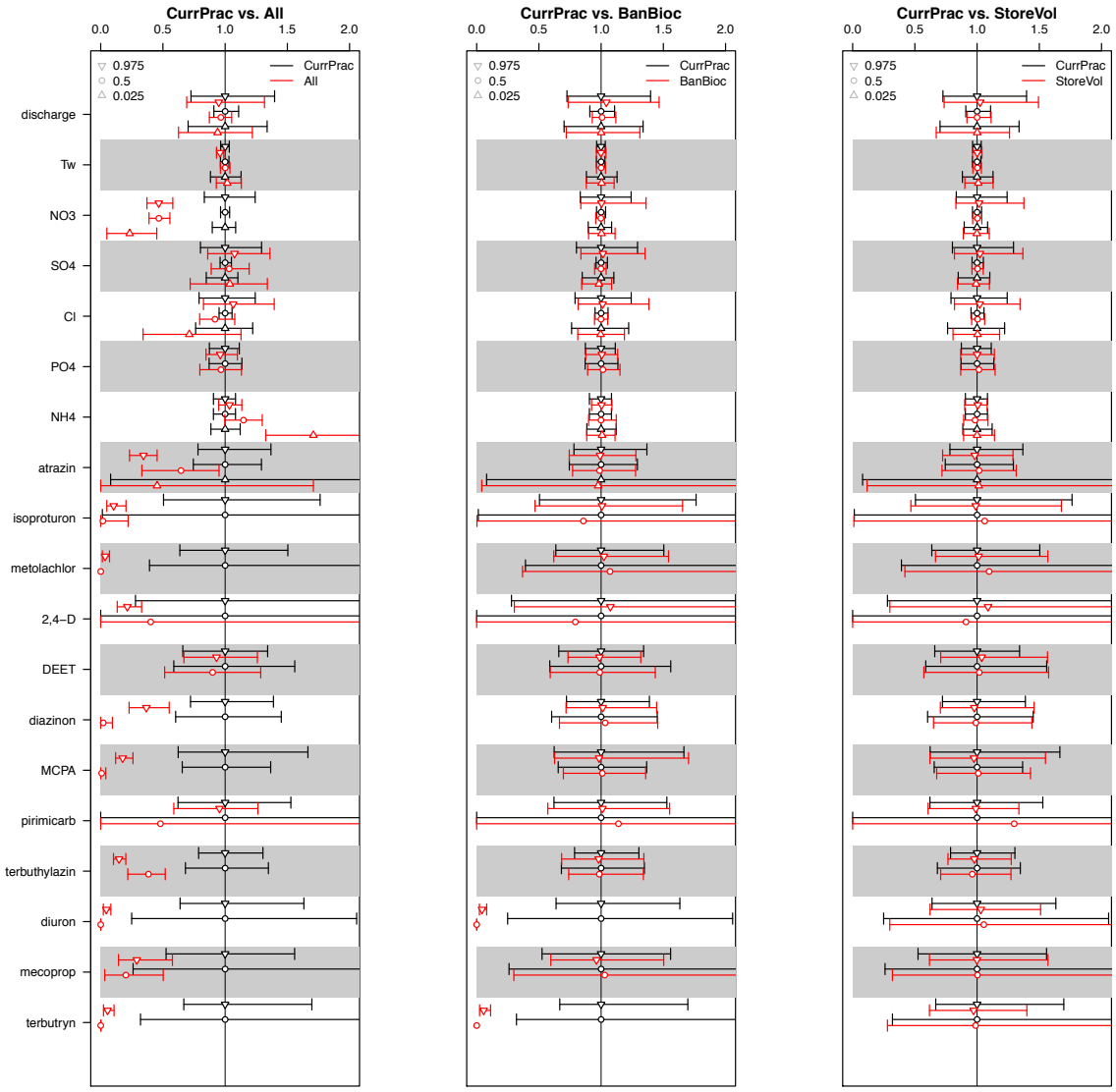

Figure S9: Relative change for high (Q97.5%), median (Q50%) and low (Q2.5%) quantiles of predicted model variables. Unless otherwise stated, all simulations used present climate + StatusQuo + CurrPrac. Missing low quantiles correspond to cases where a present expected value of 0 for the low quantile prevented the meaningful normalisation of values.

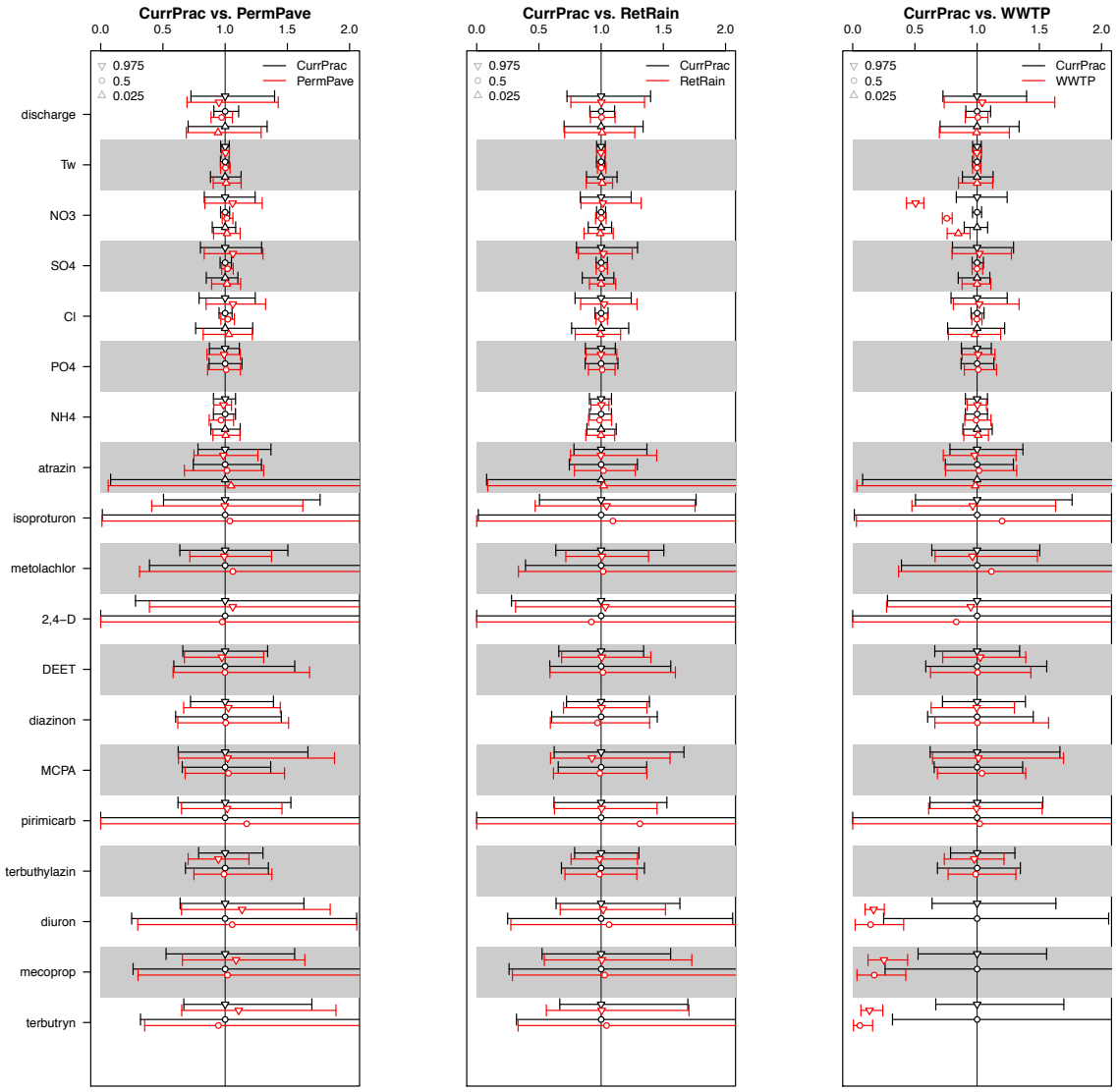

Figure S10: Relative change for high (Q97.5%), median (Q50%) and low (Q2.5%) quantiles of predicted model variables. Unless otherwise stated, all simulations used present climate + StatusQuo + CurrPrac. Missing low quantiles correspond to cases where a present expected value of 0 for the low quantile prevented the meaningful normalisation of values.

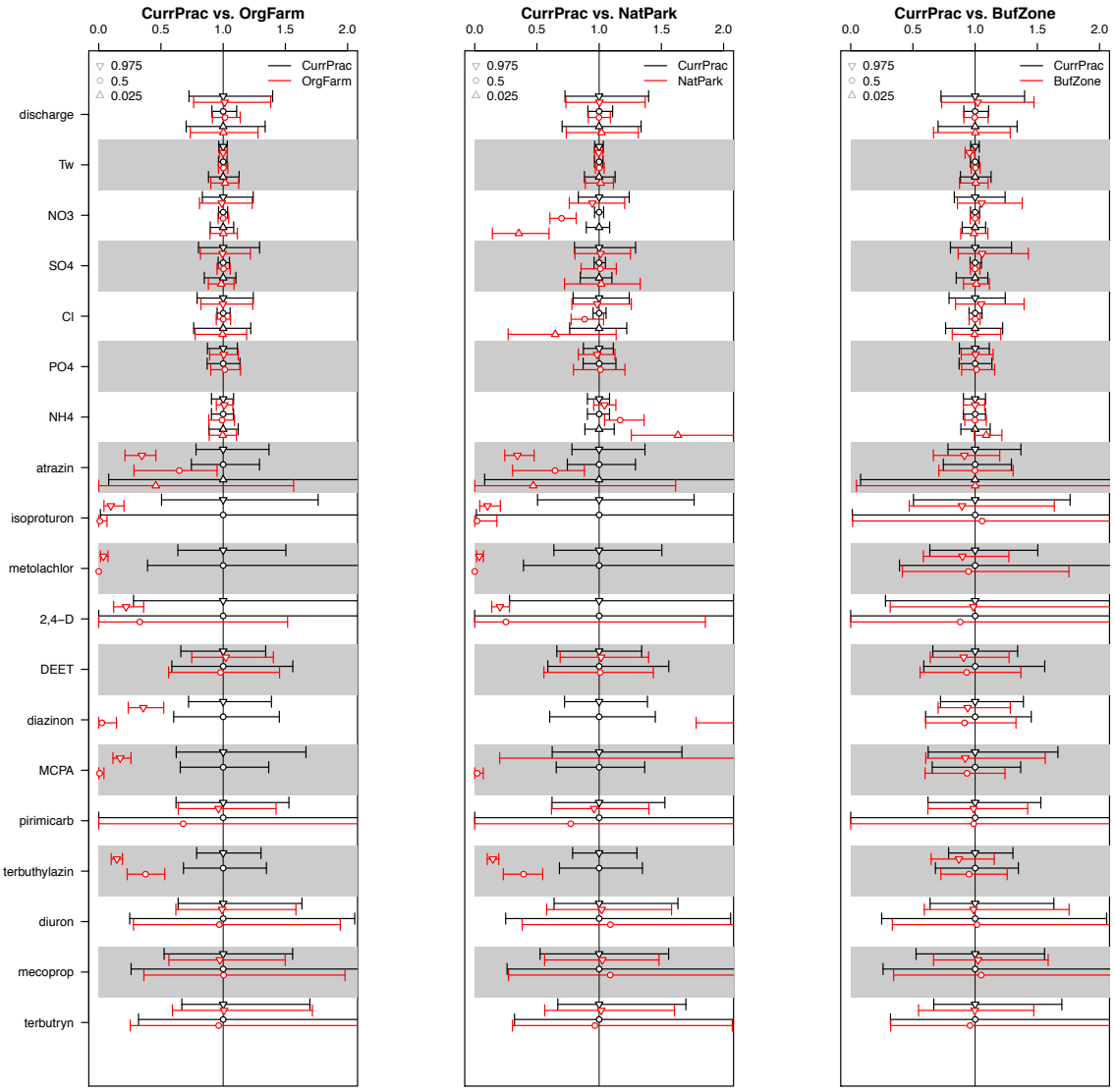

Figure S11: Relative change for high (Q97.5%), median (Q50%) and low (Q2.5%) quantiles of predicted model variables. Unless otherwise stated, all simulations used present climate + StatusQuo + CurrPrac. Missing low quantiles correspond to cases where a present expected value of 0 for the low quantile prevented the meaningful normalisation of values.

The full version of Table 6 of the main manuscript is shown below featuring all modelled PPPs and biocides:

	Physical parameters and pollutant concentrations													
Management measure	Q	T	Atrazine	Isoproturon	Metolachlor	2,4-D	DEET	Diazinon	MCPA	Pirimicarb	Terbuthylazin	Diuron	Mecoprop	Terbutryn
All	–	–	–	–	–	–	–	–	–	–	–	–	–	–
BanBioc	0	0	0	0	0	0	0	0	0	0	0	–	0	–
StoreVol	0	0	0	0	0	0	0	0	0	0	0	0	0	0
PermPave	–	0	0	0	0	0	0	0	0	0	0	–	–	–
RetRain	–	0	0	0	0	0	0	0	0	0	0	–	0	–
WWTP	0	0	0	0	0	0	0	0	0	0	0	–	–	–
OrgFarm	0	0	–	–	–	–	0	–	–	–	–	0	0	0
BufZone	0	–	–	–	–	–	–	–	–	0	–	0	0	0
NatPark	0	0	–	–	–	–	0	–	±	–	–	0	0	0